# Surfactants for $CO_2$ - Supporting Information

Julian Eastoe*[☯], Sarah Gold[☯], David C Steytler[♦]

[☯]*School of Chemistry, University of Bristol, Bristol, BS8 1TS, United Kingdom,*
[♦]*School of Chemical Sciences and Pharmacy, University of East Anglia, Norwich NR4 7TJ, United Kingdom.*

## 1. Surfactant synthesis

The synthetic procedures and methods of chemical characterization for the compounds listed in Table 1 of the manuscript are given in the appropriate papers: surfactants **1** [1, 2], **2** [3, 4], **3** [5], **4** [6], **6** [7] and **7** [8]. As an example of the tri-chain series **5,** synthetic details for TCS-4 (Scheme S1).

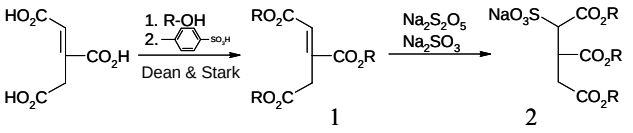


**Scheme 1.** Synthesis of tri-chain $CO_2$-philic surfactants.

*Synthesis of (E)-3-(2,2-Dimethyl-propoxycarbonyl)-pent-2-enedioic acid bis-(2,2-dimethyl-propyl) ester (1)*
Trans-aconitic acid (5 g, 28.75 mmol) and neo-pentyl alcohol (3.2 eq., 8.07 g, 92 mmol) was dissolved in toluene (100 ml) and p-toluene sulfonic acid (0.99g, 5.75 mmol) added. The reaction mixture was heated to 110 °C for 12 h and water generated removed via Dean and Stark apparatus. The reaction mixture was washed repeatedly with saturated $NaHCO_3$ (aq) solution, the organic phase dried over $MgSO_4$ and solvent removed to give an off white oil. Purification was achieved via flash column chromatography over $SiO_2$ using 10% $Et_2O$/Petroleum Ether. $^1$H NMR ($CDCl_3$): (δ=0.97) C(C**H**$_3$)$_3$, (δ=3.77,3.88,3.90) $CO_2$C**H**$_2$, (δ=4.02) C**H**$_2$CO$_2$, (δ=6.99) C=C**H**-
Yield: 78%.

*Synthesis of Sodium; 1,2,3-tris-(2,2-dimethyl-propoxycarbonyl)-propane-1-sulfonate (2)*
Triester (1) (8.3 g, 22.4 mmol), was dissolved in ethanol (100ml) and water added up to saturation. $Na_2S_2O_5$ (2.2 eq., 9.37 g, 49.3 mmol), $Na_2SO_3$ ( 1.8 eq., 5 g, 40.3 mmol) was then added and the mixture was allowed to heat under reflux for 6 h. Solvent was completely removed to give white solid product which underwent crude purification via Sohxlet extraction using dry distilled AcOEt. Further purification was achieved by dissolving in the minimum amount of dry MeOH and spinning resultant solution in a centrifuge at 6000 rpm for 30 min. The supernatant solution was decanted from residual salts and solvent removed to yield white solid. $^1$H NMR: (δ=0.97) C(C**H**$_3$)$_3$, (δ=3.68-3.90) $CO_2$C**H**$_2$, (δ=3.95) C**H**$_2$CO$_2$, (δ=3.22) C**H**-, (δ=4.49) $NaO_3$S-C**H**-
Yield: 56%

## 2. Surfactant purity.

A feature of the work described in the main article has been the use of research grade, custom-synthesized surfactants, of high surface chemical purity. In this respect the work is distinguished from the majority of other published literature in the field, which has tended to employ commercial or technical grade compounds. High surface chemical purity is known to be an essential pre-requisite for meaningful studies of air-water [9, 10] and oil-water interfaces [11-13]. Post-synthesis treatment methods for obtaining surface chemically pure surfactants used to formulate $CO_2$ microemulsions are described elsewhere [4, 6, 9, 10, 13].

A stringent test applied in this work is quantitative comparison of pre-cmc surface excesses (Γ) determined by two independent methods: drop volume surface tensiometry (DVT) and neutron reflection (NR). Experimental details of these methods, and explanation of why they are appropriate for this task, are outlined in accompanying references [4, 6, 9, 10, 13]. Figure S1 shows an example of this test of surface chemical purity for two anionic $CO_2$ surfactants from classes Ia (di-HCF4) and Ib (di-CF4): similar checks have been made for other surfactants prior to studies in $CO_2$.

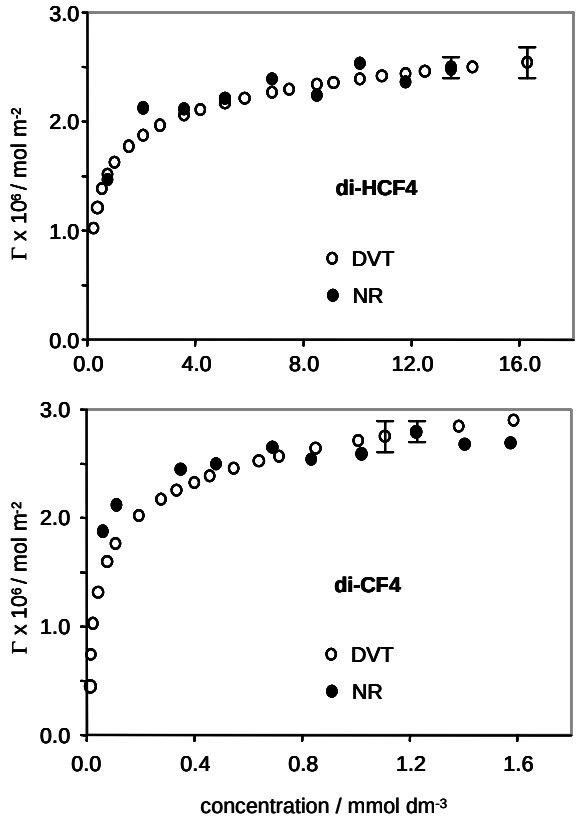


**Figure S1.** Test for surface chemical purity of $CO_2$-philes. Comparison of adsorption isotherms derived from drop volume surface tension (DVT, O) measurements and neutron reflection (NR, ●) for example $CO_2$-philes di-HCF4 and di-CF4. [2]

## 3. Scattering and spectroscopic techniques

*Near Infra-red spectroscopy*

Near Infra-red spectra of binary surfactant/$CO_2$ mixtures, water/surfactant/$CO_2$ and water/surfactant/alcohol/$CO_2$ phases were obtained using a Thermo-Nicolet Nexus spectrometer comprising a DTGS detector and a tungsten lamp. Appropriate background spectra were obtained for subtraction. Great care was taken to ensure that no water droplets or surfactant-supported film were present on the cell windows during data acquisition, as this would lead to erroneous detection of bulk water in the NIR spectra. For solubility tests with binary mixtures, excess surfactant was placed in a custom-made gauze attached to the piston inside the pressure cell. The cell was filled with $CO_2$, stirred (two magnetic fleas) then allowed to equilibrate

for 30 min., then aligned in the spectrometer using an x/y/z translation stage. The spectrum was recorded after any excess solids had settled. For the ternary and quaternary mixtures, samples were pre-formulated and equilibrated off-line, with P-T control and stirring to achieve single phases, prior to alignment in the spectrometer. Spectral data handling and background subtractions were carried out using OMNIC version 5.12 software.

*High-pressure Small-angle Neutron Scattering (HP-SANS)*

Small-angle neutron scattering (SANS) was used to characterize the water-in-$CO_2$ microemulsion structure. Experiments were conducted on the time-of-flight small-angle diffractometer LOQ at ISIS, Rutherford Appleton Laboratory, Didcot, UK [14, 15], in conjunction with the pressure cell described elsewhere [16]. A 12 mm path length was required to optimize sample transmission. $D_2O$ was used to provide contrast to size the aqueous water pools of the reversed microemulsion droplets. Neutron counts were accumulated over periods of 60 minutes to provide data of sufficient statistical quality, and 10-minutes were allowed for transmission runs.

Standard procedures [e.g.15] for the normalization of raw neutron counts as a function of wavelength λ = 2.2 to 10 Å yielded normalized scattering intensities $I(Q)$ in $cm^{-1}$, where the momentum transfer, $Q = (4\pi/\lambda)\sin(\theta/2)$ and θ is the scattering angle (<7°). Scattering data were corrected for wavelength-dependent transmission factors, background (empty cell and $CO_2$) and hydrocarbon incoherent scattering arising from hydrogen in the surfactant [15]. Intensities were also corrected for path length, P-T induced changes in sample volumes, allowing for various conditions to be compared [17].

**4. Spherical core-shell form factor**

For polydisperse, homogeneous spherical particles the SANS intensity $I(Q)$ / ($cm^{-1}$) is given by,

$$I(Q) = N_P\,[P(Q,R)\;p(R)]\;S(Q) + B_{inc} \qquad (A1)$$

where $I(Q)$ is the absolute scattering intensity, $N_P$ is the particle number density, $P(Q)$ is the single particle form factor, $p(R)$ is a normalized distribution function, $S(Q)$ is the interparticle structure factor, which accounts for interactions. The level $B_{inc}$ represents a sample-dependent isotropic incoherent background, which is determined by independently measuring the $CO_2$ solvent for subtraction from the sample + solvent data.

For core-shell spherical particles the general form factor $P(Q,R)$ is given by [18]

$$P(Q,R) = \frac{16\pi^2}{9}\left[(\rho_{shell}-\rho_{solv})\,3R_D^3\left(\frac{\sin QR_D - QR_D\cos QR_D}{(QR_D)^3}\right) - 3r_C^3\left(\frac{\sin QR_C - QR_C\cos QR_C}{(QR_C)^3}\right)\right]^2 +$$

$$(\rho_{core}-\rho_{solv})\,3R_C^3\left(\frac{\sin QR_C - QR_C\cos QR_C}{(QR_C)^3}\right)\Bigg]^2 \qquad (A2)$$

where $R_D$ is the droplet radius, $R_C$ the core radius. In line with the configuration presented in Figure 7b of the main paper, the parameters $\rho_{solv}$, $\rho_{shell}$, $\rho_{core}$ represent the coherent scattering length densities (*sld*) of the $CO_2$ medium, surfactant shell, and $D_2O$ core respectively. The interfacial adsorbed layer thickness $T$ is given by $R_D$—$R_C$. With dilute core-shell particles (volume fraction < 0.05) Ottewill *et al.* [18] were the first to show that a peak can arise in $I(Q)$, originating from the form factor only; note that this $P(Q)$ peak is distinct from any interparticle interferences that are normally manifest in the structure factor $S(Q)$.

For dilute water-in-$CO_2$ systems which are located away from phase boundaries (e.g. Figures 6 and 7a in the main paper), and show no evidence for attractive $S(Q)_{ATT}$ in the scattering (absence of low $Q$ critical scattering), no $S(Q)$functions were needed in the analysis. Since the volume fraction concentrations studied here are low (< 0.05), to a good first approximation volume exclusion inter-particle interactions (hard-sphere structure factor $S_{HS}(Q)$) may be safely neglected. To test for this, trial fits to the data in Figure 7b of the main paper were carried out; including appropriate $S_{HS}(Q)$ functions, gave essentially the same structural parameters for the core-shell droplets as without $S_{HS}(Q)$, and so in final analyses the structure factor was omitted.

For systems where attractive interactions have to be considered, particularly in the vicinity of phase boundary or phase separation region in binary solutions, an Ornstein-Zernicke structure factor $S(Q)_{ATT}$ can be included in the scattering law [19]. This function describes a decaying particle distribution with correlation length ζ. Far from phase boundaries, $S(0)\rightarrow 0$, and then $S(Q)_{ATT}\rightarrow 1$. For the systems under study here, this function is entirely effective, simply taking into account additional scattering at low Q. It is characterised by a correlation length ζ and $S(0)$

$$S(Q)_{ATT} = 1 + \frac{S(0)}{1+(Q\zeta)^2} \qquad (A3)$$

Quantitatively, S(0) may be related to the strength of interactions via isothermal compressibility χ,

$$S(0) = n_p\,k_B\,T\,\chi \qquad (A4)$$

A polydispersity term is included in Eq. A1. This was a Schultz distribution function, [19] defined by an average radius $\bar{R}$ and a root mean square (RMS) deviation σ given by

$$\sigma = \left[\overline{(R-\bar{R})^2}\right]^{1/2} = (\overline{R^2}-\bar{R}^2)^{1/2} = \bar{R}/(Z+1)^{1/2} \qquad (A5)$$

where Z is a width parameter. The polydispersity reported in the main paper is $\sigma / \bar{R}$. The SANS data were fitted using the interactive FISH program [20], which is a flexible multi-model package comprising a variety of different form factors $P(Q)$, structure factors $S(Q)$, and polydispersity functions. Extensive fitting trials, with different scattering laws, yield the most appropriate model: this procedure is outlined in references 4 a and 4b.

**5. The "fingerprint" SANS curve for core-shell droplets**

Using the form factor given above simulations were performed to explore the effects of changing; (a) internal core radius $R_c$ (Figure S2), (b) surfactant shell thickness T (Figure S3) and (c) solvent scattering length density $\rho_{solv}$ (Figure S4). In these calculations the polydispersity $\sigma / \bar{R}$ was fixed at 0.15 and the volume fraction was 0.05.

Figures S2-S4 reveal the sensitivity of the core-shell form factor to changes in all three parameters, which are important for characterizing surfactant-stabilized nanodroplets in $CO_2$.

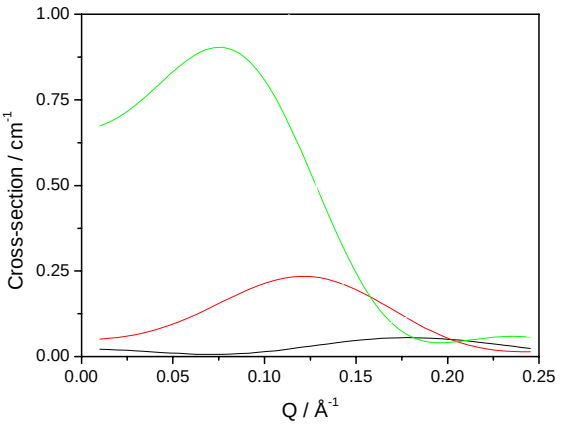


**Figure S2**: Form factor calculations with scattering length densities 2.4, 0.3 and 6.4 x $10^{10}$ $cm^{-2}$ for the external $CO_2$ phase, shell and $D_2O$ core respectively, and a layer thickness T = 8 Å. The internal $D_2O$ core radius is 15 Å (black), 20 Å (red) and 25 Å (green).

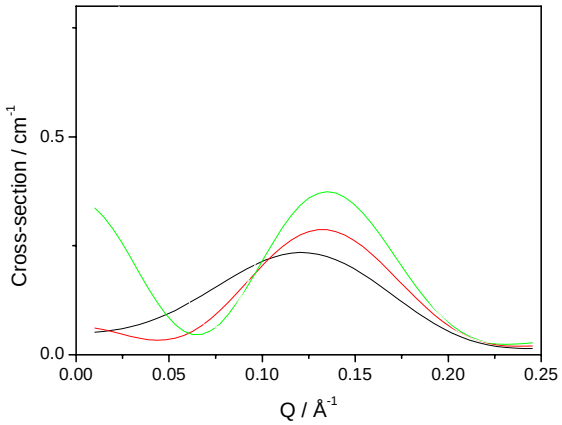


**Figure S3**: Form factor calculations with scattering length densities 2.4, 0.3 and 6.4 x $10^{10}$ $cm^{-2}$ for the external $CO_2$ phase, shell and $D_2O$ core respectively, and an internal $D_2O$ core radius of 20 Å. The layer thickness T is 8 Å (black), 10 Å (red) and 12 Å (green).

Based on these simulations it can be seen that SANS offers a unique opportunity to experimentally simulate the *I(Q)* signal, expected if any given surfactant were to aggregate or microemulsify water in $CO_2$. Because the scattering length density $\rho_{solv}$ of liquid $CO_2$ at a typical mass density of 1 g $cm^{-3}$ is 2.5 x $10^{10}$ $cm^{-2}$ [21], it is possible to formulate a suitable mixture of hydrogen-containing and deuterated hydrocarbon solvents to provide the same value of $\rho_{solv}$. Since most non-ionic surfactants are highly soluble in cyclohexane, this was chosen as a model solvent.

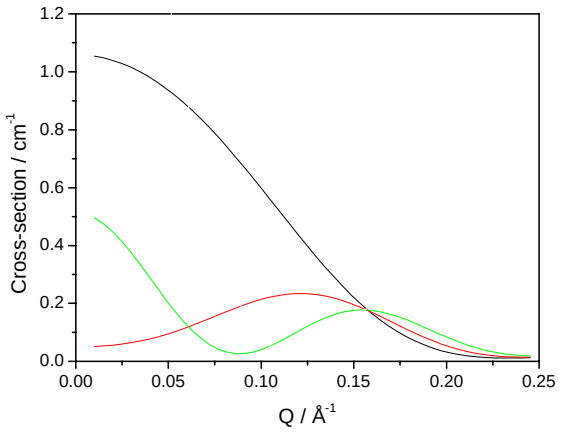


**Figure S4**: Form factor calculations with scattering length densities 0.3 and 6.4 x $10^{10}$ $cm^{-2}$ for the shell and $D_2O$ core respectively, an internal $D_2O$ core radius of 20 Å and a layer thickness T 8 Å. The scattering length density of the external solvent $\rho_{solv}$ is 1.2 (black), 2.4 (red) and 3.6 (green) in units of x $10^{10}$ $cm^{-2}$.

A mixture containing 40% volume of $C_6D_{12}$ (Goss, 99.8% D-atom, $\rho_{solv}$ = +6.7 x $10^{10}$ $cm^{-2}$) and 60% volume of $C_6H_{12}$ (Aldrich, 99.9%, $\rho_{solv}$ = -0.28 x $10^{10}$ $cm^{-2}$) results in a net solvent scattering length density matched to that of $CO_2$ i.e. 2.5 x $10^{10}$ $cm^{-2}$ (of course $\rho_{CO2}$ is pressure and temperature sensitive, but in the liquid region around 1 g $cm^{-3}$ there are only small effects [21]). Thus, using this 4:6 D/H cyclohexane mixture as the continuous solvent and measuring SANS from model water-in-oil (w/o) systems, the scattering profile expected for any given $D_2O$ core/H-surfactant shell/"$CO_2$" microemulsion droplets can be simulated. This type of SANS profile is, therefore, characteristic and can be used as a diagnostic test when compared to the SANS signals observed in real water-in-$CO_2$ dispersions.

Test SANS experiments were carried out at the D22 diffractometer at ILL (Grenoble, France) using a neutron wavelength $\lambda$ = 10 Å at two different detector distances to cover a Q range of 0.0024 → 0.37 $Å^{-1}$, and also at the time-of-flight LOQ instrument at ISIS, UK where incident wavelengths are 2.2 ≤$\lambda$≤ 10 Å, resulting in an effective Q range of 0.009 → 0.249 $Å^{-1}$. Measurements were conducted in 2 mm rectangular quartz cells. The sample compositions were defined by the surfactant concentration in % w/v and the water loading w = $[D_2O]/[surf]$.

Figures S5-S7 show the evolution of the SANS profiles, as a function of added $D_2O$ (increasing w) with model non-ionic surfactant Triton X45 (Aldrich) at constant concentration, stabilizing microemulsion droplets in the 4:6 D/H cyclohexane mixture, which simulates liquid $CO_2$. It is clear that swelling of the reversed micelles by addition of $D_2O$ caused dramatic changes: the aggregate dimensions become enlarged, which also introduces a core-shell contrast, resulting in the appearance of a clear peak in the form factor for $w$ = 6 (Figure S7). The data were fitted by the model given in section 3, but modified to give an extra contrast step: radius of the water core ($R_C$), length of the hydrated EO chain ($T_{EO}$) and length of the octyl-phenyl hydrophobe ($T_{tail}$). The parameters used, with polydispersity index ($\sigma$ / $\overline{R}$ $r$ = 0.20) are given below in Table S1, together with the corresponding *sld* values.

| $w$ | $R_C$ (Å) | $T_{EO}$ (Å) | $T_{tail}$ (Å) |
|---|---|---|---|
| 3 | 17.5 (6.4) | 8.8 (2.5) | 8.0 (0.4) |
| 6 | 23.7 (6.4) | 8.8 (2.5) | 8.0 (0.4) |

**Table S1**: Parameters used to fit low-$w$ microemulsions formed by Triton X45 in a 4:6 $C_6D_{12}/C_6H_{12}$ mixture simulating $CO_2$. Fitted ρ values given in brackets x $10^{10}$ $cm^{-2}$.

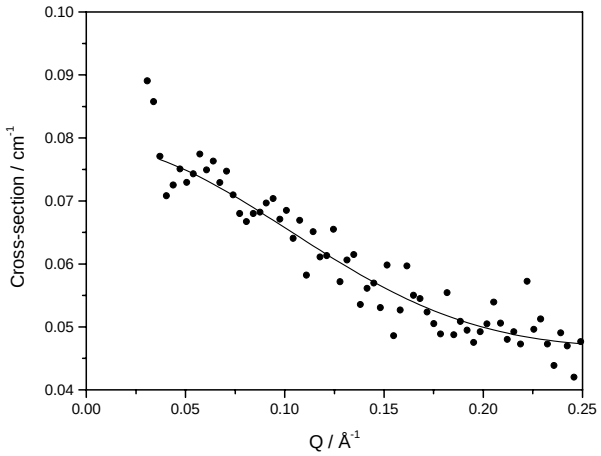


**Figure S5**: SANS data for w = 0 reversed micelles of Triton X45 (5% w/v; w = 0) in a 4:6 $C_6D_{12}/C_6H_{12}$ mixture at 25°C; the symbols are SANS data, and the line is the model fit for a homogenous polydisperse sphere of r = 14 Å and polydispersity 0.20.

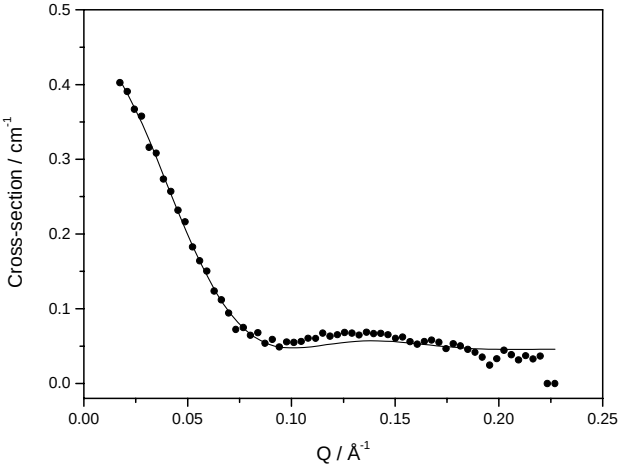


**Figure S6**: SANS data from a Triton X45 (5% w/v; w = 3) w/o microemulsion in a 4:6 $C_6D_{12}/C_6H_{12}$ mixture at 25°C; the symbols are SANS data and the line is the model fit.

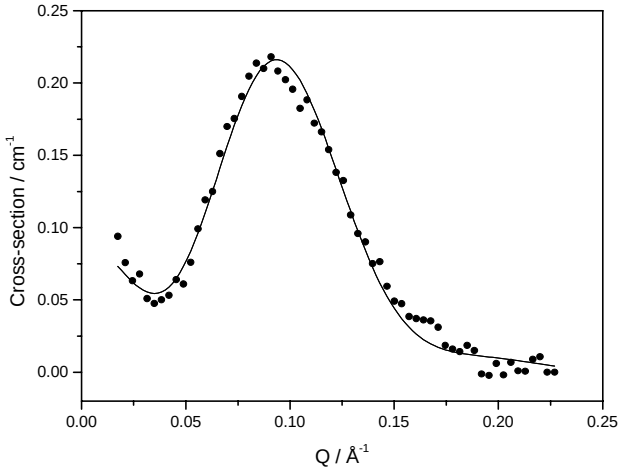


**Figure S7**: SANS data from a Triton X45 (5% w/v; w = 6) w/o microemulsion in a 4:6 $C_6D_{12}/C_6H_{12}$ mixture at 25°C; the symbols are SANS data and the line is the model fit. The peak originates from the *P(Q)* form factor and intraparticle interference effects, rather than an interparticle structure factor *S(Q)*.

Interestingly, Figure S7, shows the clear "fingerprint" form factor peak for SANS from a core-shell structure, with a similar configuration to that given in Figure 7a of the main paper.

### 6. Evaluation of potential and previously claimed stabilizers for w/c systems

HP-SANS experiments were performed on $D_2O$ and $CO_2$ systems, with likely candidate surfactants, and also those for which claims of stabilization had previously been made [21-24]. In these investigations surfactant levels, water concentrations, $CO_2$ pressure and temperature were all systematically varied (surfactant 1-10 wt%, w 0 – 20, T 15-50°C, P 50-500 bar). More detail on these experiments can be found elsewhere [25, 26].

a. Triton non-ionics

Triton X100, Triton X100(reduced) and Triton X45 (all from Aldrich) were all evaluated. Although small changes in the SANS amplitude could be detected on injection of water into Triton non-ionics in $CO_2$ (data not shown), no such responses as given in Figures S2-S4 or S7 were obtained, only very low scattering. The best case scenarios gave weak *I(Q)* curves similar to Figure S4, suggesting that true w/c microemulsions cannot be stabilized by these hydrocarbon non-ionic surfactants.

b. Tergitol® Surfactants

Tergitol® surfactants form a class of non-ionic hydrocarbon surfactants possessing a branched 2,6,8-trimethyl-4-nonyl hydrophobe. Stabilization of w/c microemulsions stabilised by Tergitol TMN 6 (Fluka, MW 553, and average ethylene oxide number 8.3, HLB 13.1) has been claimed [22]. However the surfactant concentration employed was low such that the w-values were close to, or even below, the levels of water required to saturate the $CO_2$ phase itself. The possible formation of w/c microemulsions was therefore tested using the SANS approach outlined above. Before use TMN6 was dried in a desiccator over phosphorous pentoxide for two weeks.

Figures S8 and S9 show test SANS experiments using the 4:6 D/H cyclohexane solvent mixtures. These data were analysed by the core-shell model described above; fitted parameters are given in Table S2 and the functions are shown on the figures. In this case the core region only appears to be comprised of hydrated EO chains.

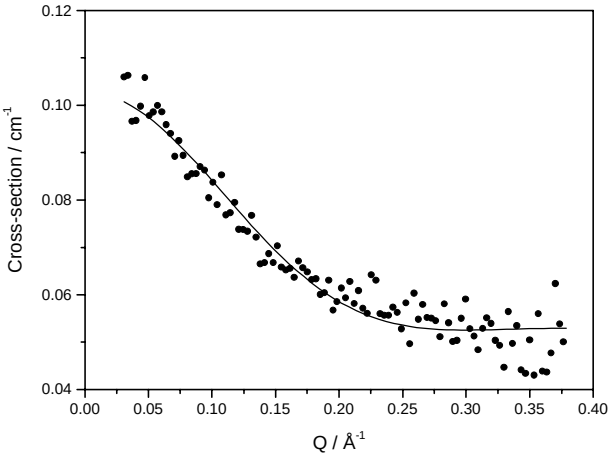


**Figure S8:** SANS data from Tergitol TMN 6 (5% w/v; w = 0) reversed micelles in a 4:6 $C_6D_{12}/C_6H_{12}$ mixture at 25°C; the symbols are SANS data and the line is the model fit.

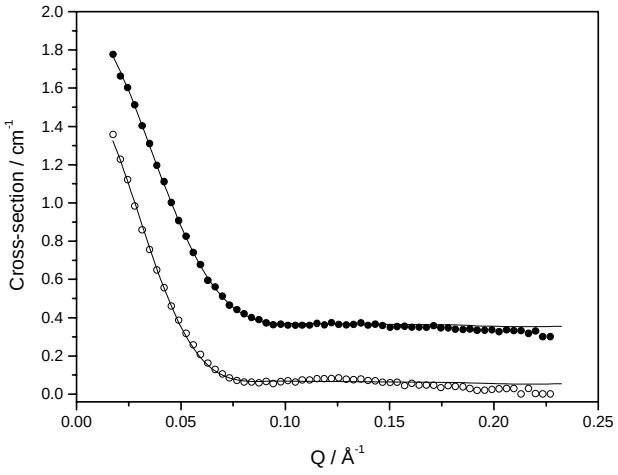


**Figure S9**: SANS data from Tergitol TMN 6 (5% w/v) reversed micelles in a 4:6 $C_6D_{12}/C_6H_{12}$ mixture at 25°C; approximate water content (w value): (●) w = 3; (○) w = 6; the symbols are SANS data and the lines are model fits.

| *w* | *r* (Å) | *T* (Å) |
|---|---|---|
| 0 | 5.5 (0.4) | 9 (0.4) |
| 3 | 28 (1.3) | 9 (0.4) |
| 6 | 34 (1.9) | 9 (0.4) |

**Table S2**: Parameters used to fit low-w microemulsions formed by Tergitol TMN 6 in a 4:6 $C_6D_{12}/C_6H_{12}$ mixture. Numbers quoted in brackets represent ρ values in $10^{10}$ $cm^{-2}$.

Next $D_2O$-TMN 6-$CO_2$ mixed systems were interrogated by HP-SANS, the measured *I(Q)* data and analyses are shown in Figure S10. The response to water injection appears to enhance micelle formation in $CO_2$, possibly through H-bonding interactions with low levels of water hydrating the EO chains. However, there was no indication of true w/c microemulsion formation by this surfactant. The data were fitted to a Schulz polydisperse sphere model [17, 18]. With increasing w value the data give some suggestion of an increase in amplitude and radius (from ~12.0 Å to ~16.0 Å) but intensities were still low, and the higher *w*-values are certainly not typical of microemulsion systems in $CO_2$. Importantly, none of the curves in Figure S10 bear any resemblance to the "expected" scattering shown in Figures S2-S4 and S7.

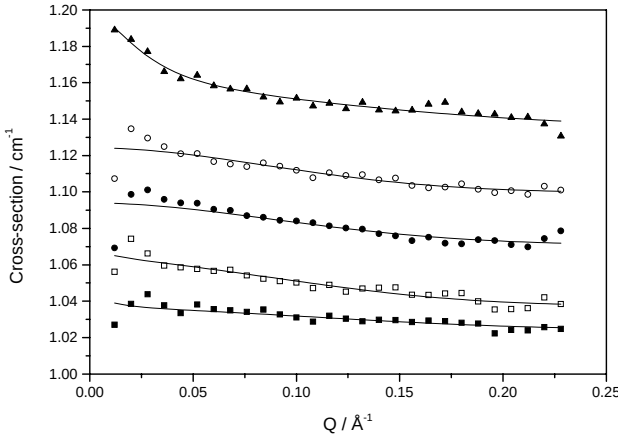


**Figure S10:** SANS data from water-$CO_2$ mixtures in the presence of Tergitol TMN 6 at 50°C and 500 bar; approximate water content (w value): (■) *w* = 0; (□) w = 2.9; (●) w = 5.8; (○) w = 8.7; (▲ ) w = 11.6; the symbols are SANS data and the lines are model fits to a polydisperse sphere model [17, 18]. The curves are shifted vertically for clarity of presentation.

c. Dynol Surfactants

Dynol surfactants are a series of 2,5,8,11-tetrametyl-6-dodecyn-5,8-diol ethoxylate non-ionic hydrocarbon surfactants possessing a methylated acetylenic structure. It has been claimed that surfactants from this class, like Dynol 604, stabilize water-in-$CO_2$ microemulsions [23]. Figures S11 and S12 show results of HP-SANS experiments with this compound. As was indicated for Tergitol TMN 6, added water appears to induce micelle formation probably by increasing hydrogen bonding in the core. However, the data do not resemble those expected for a true w/c microemulsion of this water content. It was found that Dynol 604 does not stabilise microemulsions in cyclohexane, so the approach adopted previously to simulate scattering from a "$CO_2$-like" oil medium could not be applied here.

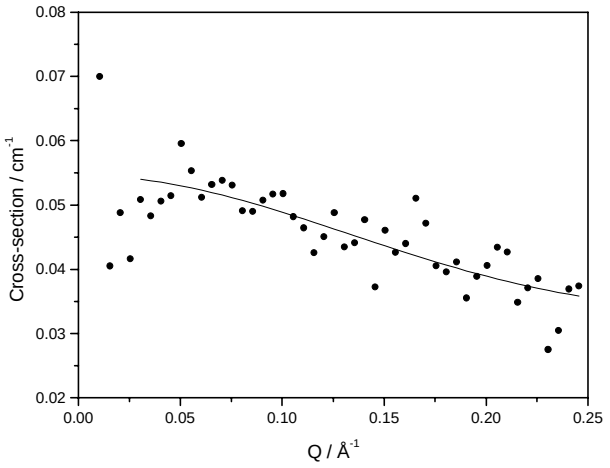


**Figure S11**: SANS data from a Dynol 604 (~ 5 wt %) solution in carbon dioxide taken at 35°C and 360 bar.

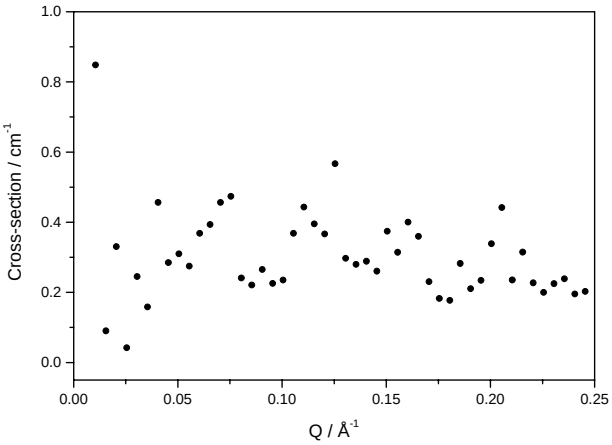


**Figure S12**: SANS data of a Dynol 604 (~ 5 wt %) and $D_2O$ (200 μL) mixture in carbon dioxide taken at 35°C and 450 bar. Line is fit to a polydisperse sphere model giving a mean radius of ~11.0 Å for the micelles, and polydispersity 0.22.

*d. Mixed AOT-alcohol systems*

It has been claimed [24] that mixtures of normal AOT and n-hexanol stabilize w/c droplets, with the pentanol acting as a co-surfactant. In to this concept of enhanced water miscibility in $CO_2$ with a regular commercially available surfactant, promoted by a medium chain length alcohol it was decided to study water uptake with the $CO_2$-philic AOT4 and the precursor alcohol 3,5,5-trimethyl-1-hexanol. More detail can be found in reference 25. The rationale being that AOT4 would be a better choice than AOT, owing to proven enhanced compatibility with the solvent (main paper). Dispersions of water stabilized by AOT4 (IV in the main paper) in 3,5,5-trimethyl-1-hexanol/$CO_2$ mixed solvent systems were examined. Due to the lack available data, w values could not be corrected for the solubility of water in the solvent mixture of 3,5,5-trimethyl-1-hexanol and $CO_2$ over the P-T range studied. Nevertheless, it is worth noting that water appeared to be insoluble in 3,5,5-trimethyl-1-hexanol at room temperature and atmospheric (ambient) pressure. When water was added to a solution of AOT4 at a concentration of 0.03 mol $dm^{-3}$ in a mixture of $CO_2$/3,5,5-trimethyl-1-hexanol (the amount of alcohol varying from 5 to 12 mol%), optically transparent single phases were quickly formed. Background experiments were conducted with solely water/*sc*-$CO_2$ and alcohol. In the absence of AOT4, water could not be dispersed into a transparent single phase.

Cloud point data as a function of added water are shown in Figure S13; the system composition was 0.03 mol $dm^{-3}$ AOT4 in 12 mol% alcohol-modified $CO_2$ solvent mixture. Transition pressures were uncharacteristically low for surfactant stabilized systems in $CO_2$. For instance, single phases, with water content varying from w = 10 to 30, were stable at 25 °C and below 90 bar!

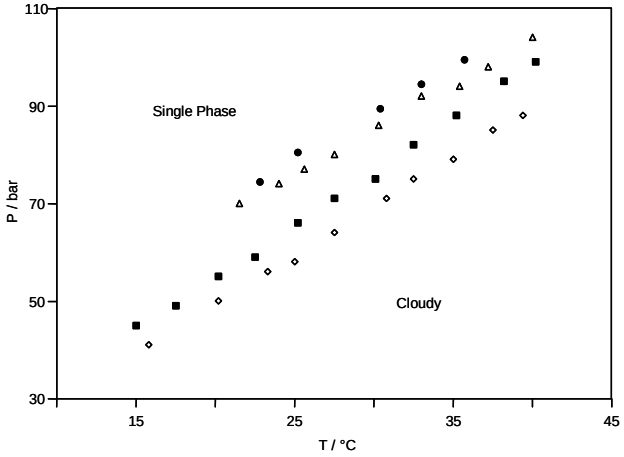


**Figure S13** P-T phase diagram as a function of added water: (◊) w = 0, (■) w = 10, (△) w = 20 and (●) w = 30. Dispersions were stabilized by 0.03 mol $dm^{-3}$ AOT4 in a solvent mixture of liquid $CO_2$/3,5,5-trimethyl-1-hexanol in the proportions 88:12 (mol/mol).

NIR spectroscopy was used to provide indirect evidence for dispersed water in these systems. Spectra of water/AOT4/$CO_2$/alcohol systems were acquired at 300 bar and 30 °C. Spectral profiles obtained after subtraction of the $CO_2$ background are shown in Figure S14; the surfactant concentration was 0.03 mol $dm^{-3}$, the alcohol content was 12 mol% and w was varied between 0 and 30. NIR data at w = 0 displayed a sharp, well-resolved band at ~ 1390 nm, which corresponds to the O-H adsorption of alcohol molecules dispersed in a $CO_2$ bulk phase. Upon addition of water, an extra broad band centered on 1440 nm appeared. This band is characteristic of the υ(O-H) stretching mode, where the width of the band indicates hydrogen-bonded environments. The intensity and the area of the bands at 1390 nm and 1440 nm increased with added water, strongly suggesting that water was dispersed both in the bulk $CO_2$ phase and in a polar environment via hydrogen bonding.

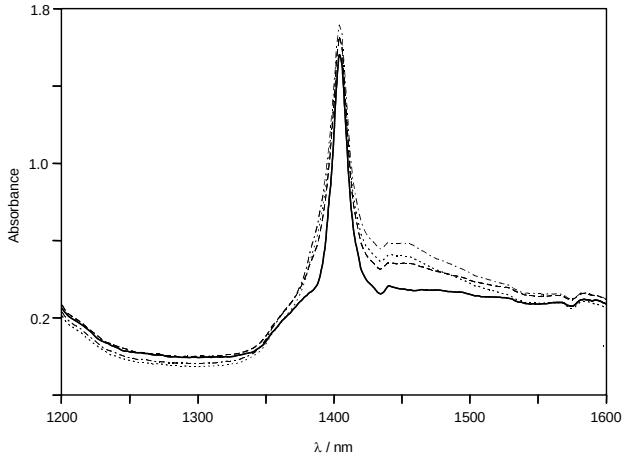


**Figure S14** NIR spectra as a function of added water: (--) w = 0, (---) w = 10, (···) w = 20 and (-·-) w =30. Dispersions were stabilised by 0.03 mol $dm^{-3}$ AOT4 in a mixture of solvents, $CO_2$/3,5,5-trimethyl-1-hexanol in the proportions 88:12 (mol/mol). Spectra were acquired at 300 bar and 30 °C, corresponding $CO_2$ backgrounds were subtracted.

In Figure S15, characteristic O-H adsorption modes of water dispersed in the $CO_2$/3,5,5-trimethyl-1-hexanol solvent mixture (12 mol% alcohol) may be observed. These spectra were obtained by subtraction of the background spectrum at w = 0 in Figure S14 from the spectral data at w = 10, 20 and 30. As previously, spectral bands at 1390 nm and 1440 nm were observable, the intensities of which increased with added water. These data confirmed that water was present both as single molecular entities in the $CO_2$ bulk phase and as bulk water in a polar environment, which hopefully can be assimilated to a microemulsion system with micropolar water pools.

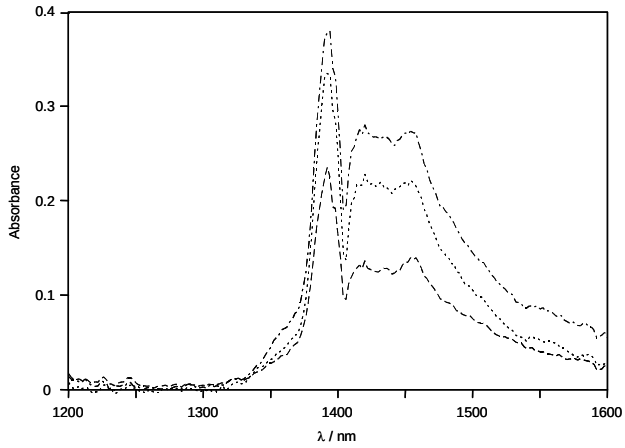


**Figure S15** NIR spectral bands of water dispersed in $CO_2$/3,5,5-trimethyl-1-hexanol solvent mixture (88:12 mol/mol) at 300 bar and 30 °C. AOT4/$CO_2$/alcohol background was subtracted.

Aggregation behavior of these systems was investigated by the direct method of high-pressure SANS. Figure S16 shows the scattering profiles of a dispersion of $D_2O$ (w = 30) stabilized by 0.03 mol $dm^{-3}$ of AOT4 in $CO_2$/3,5,5-trimethyl-1-hexanol (12 mol% alcohol), and of the background solvent mixture with and without AOT4. The observed scattering profiles were identical, suggesting that water in these systems was not dispersed in a characteristic microemulsion phase.

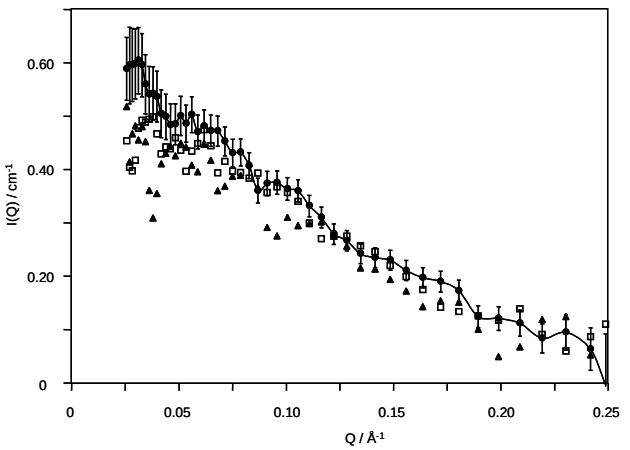


**Figure S16** SANS data of the $D_2O$/$CO_2$/3,5,5-trimethyl-1-hexanol system (w = 20) at 300 bar and 25 °C. The background systems were (□) AOT4/$CO_2$/3,5,5-trimethyl-1-hexanol and (▲) $CO_2$/3,5,5-trimethyl-1-hexanol. In each instance, the surfactant concentration was 0.03 mol $dm^{-3}$ and the solvent mixture was in the proportions 88:12 (mol/mol).

Based on these considerations, the following conclusions could be drawn. Dispersions of water in $CO_2$/3,5,5-trimethyl-1-hexanol mixtures stabilized by AOT4 could not be assigned as microemulsion phases. In previous studies of similar systems [24], fundamental evidence was lacking for the formation of microemulsions, and it can be inferred that these claims were unsubstantiated. Therefore, high-pressure SANS remains the most valuable and straightforward technique to provide clear and irrefutable evidence for microemulsion formation in $CO_2$. It is more plausible to consider these systems as homogeneous solutions without colloidal or self-assembly structures. However, this lack of nanometre-scale aggregation structure does not rule out any applications of these mixed systems as extraction medium. For example, Hutton *et al.* managed to extract various polar substances in AOT/water/$CO_2$ systems with 10 mol% pentanol at 250 bar and 40 °C [24]. It is likely that the systems described herein could serve the same purpose at even lower pressure conditions, owing to the $CO_2$-compatibility of tert-butyl units. As a conclusion, these systems appear to be the main ones, where branched derivatives of AOT could be used in applications of industrial interest.

**References**


1. Hoefling, T.A., Enick, R.M., Beckman, E.J. *J.Phys.Chem.* **1991**, *95*, 7127.
2. Downer, A.; Eastoe, J.; Pitt, A. R.; Simister, E. A.; Penfold, J. *Langmuir* **1999**, *15*, 7591.
3. Guo, W.; Li, Z.; Fung, B. M. *J. Phys. Chem.* **1992**, *96*, 6738. and Yoshino, N.; Hamano, K.; Omiya, Y. *Langmuir* **1995**, *11*, 466.
4. Eastoe, J.; Dupont, A.; Murray, M.; Martin, L.; Guittard, F.; Taffin de Givenchy, E.; Heenan, R.K. *Langmuir,* **2004***, 20,* 9953 and *Langmuir, **2004**, 20,* 9960.
5. Steytler, D. C.; Rumsey, E.; Thorpe, M.; Eastoe, J.; Paul, A.; Heenan, R. K. *Langmuir* **2001**, *17*, 7948.
6. Nave, S.; Eastoe, J.; Penfold, J. *Langmuir* **2000**, 16, 8733. and Nave, S.; Eastoe, J.; Heenan, R. K.; Steytler, D. C.; Grillo, I. *Langmuir* **2000**, 16, 8741.
7. Eastoe, J.; Gold, S.; Rogers, S.; Wyatt, P., Steytler. D.C., Gurgel, A.; Heenan, R.K.; Fan, X.; Beckman, E.J.; Enick, R.M. *Angw. Chemie* accepted 28 Feb 2006 MS # anie.200600397.
8. Fan, X.; Potluri, V.K.; McLeod, M.C.; Wang, Y.; Lui, J.; Enick, R.M.; Hamilton, A.D.; Roberts, C.B.; Johnston. J.K.; Beckman, E. J. *J.Am.Chem.Soc.* **2005**, *127*, 11754.
9. An,S.W.; ;Lu,J.R.; Thomas, R.K.; Penfold,, J. Langmuir **1996**, 12, 2446.
10. Eastoe, J.; Nave, S.; Downer, A.; Paul, A.; Rankin, A.; Tribe, K.; Penfold, J. *Langmuir* **2000**, *16*, 4511.
11. Goebel, A.; Lunkenheimer, K. *Langmuir* **1997**, *13*, 369.
12. Eastoe, J.; Atkin, R.; Hicks, S; Burnett, G.R. *Langmuir* **2004,** *20,* 5673.
13. Eastoe, J.; Gold. S.; Tabor, R. *Langmuir*, **2006**, *22*, 963.
14. Heenan, R. K. H.; Penfold, J.; King, S. M. *J. Appl. Crystallogr.* **1997**, *30*, 1140.
15. Rennie, A. R. Reduction of data from SANS instruments. In *Modern aspects of small-angle neutron scattering*; Brumberger edition; NATO ASI Series C; vol. 451; Kluwer Academic Press: USA, 1995, pp 93-105.
16. Eastoe, J.; Robinson, B.H; Steytler, D.C. *J.Chem.Soc. Faraday Trans*. **1990**, *86*, 511.
17. Paul, A. PhD Thesis University of Bristol, UK. 2001.
18. Markovic, I.; Ottewill, R.H.; Cebula, D.J.; Field, I.; Marsh, J. *Col.Polym.Sci.* **1984**, *262,* 648.
19. Kotlarchyk, M.; Chen, S-H.; Huang, J.S.; Kim, M.W. *Phys.Rev.A.* **1984**, *29,* 2054.
20. Heenan, R. K. *FISH Data Analysis Program;* Rutherford Appleton Laboratory; Report RAL-89-129; CCLRC: Didcot, U.K., **1989**, contact rkh@isis.rl.ac.uk.
21. McClain, J.B.; Londono, D.; Combes, J.R.; Romack, T.J.; Canelas, D.A.; Betts, Wignall, G.D.; Samulski, E. T.; DeSimone J.M. *J. Am. Chem. Soc.* **1996**, *118*; 917.
22. Ryoo, W.; Webber, S. E.; Johnston, K. P.; *Ind.Eng.Chem.Res*. **2003**, *42*, 6348.
23. Liu, J.; Han, B.; Zhang, J.; Li, G.; Zhang, X.; Wang, J.; Dong, B. *Chem. Eur. J*. **2002**, *8*, 1356. Liu, J.; Han, B.; Li, G.; Zhang, X.; He, J.; Liu, Z. *Langmuir* **2001**, *17*, 8040. Liu, J.; Zhang, J.; Tiancheng, M.; Han, B.; Li, G.; Wang, J.; Dong, B. *J. Supercrit. Fluid.* **2003**, *26*, 27511. Liu, J.; Han, B.; Wang, Z.; Zhang, J.; Li, G.; Yang, G. *Langmuir* **2002** *18*, 3086.
24. Hutton, B. H.; Perera, J. M.; Grieser, F.; Stevens, G. W. *Colloid Surf. A* **1999**, *146*, 227. and Hutton, B. H.; Perera, J. M.; Grieser, F.; Stevens, G. W. *Colloid Surf. A* **2001**, *189*, 177.
25. Gurgel, A.,PhD Thesis University of East Anglia, UK. 2004.
26. Dupont, A; PhD Thesis University of Bristol, UK 2004.